Physcomitrella patens MAX2 characterization suggests an ancient role for this F-box protein in photomorphogenesis rather than strigolactone signalling

Mauricio Lopez-Obando, Ruan de Villiers, Beate Hoffmann, Linnan Ma, Alexandre A. de Saint Germain, Jens Kossmann, Yoan Coudert, C. Jill Harrison, Catherine Rameau, Paul Hills, et al.

***Physcomitrella patens* MAX2 characterization**

@ijpb_fr

Physcomitrella patens MAX2 characterization suggests an ancient role for this F-box protein in photomorphogenesis rather than strigolactone signaling.

Mauricio Lopez-Obando[1, 4], Ruan de Villiers[2, 4], Beate Hoffmann[1], Linnan Ma[1], Alexandre de Saint Germain[1], Jens Kossmann[2], Yoan Coudert[3], C. Jill Harrison[3], Catherine Rameau[1], Paul Hills[2, *] and Sandrine Bonhomme[1, *]

1 Institut Jean-Pierre Bourgin, INRA, AgroParisTech, CNRS, Université Paris-Saclay, RD10, 78026 Versailles Cedex, France

2 Institute for Plant Biotechnology, Department of Genetics, Stellenbosch University, Private Bag X1, Matieland, 7602, South Africa

3 School of Biological Sciences, University of Bristol, Life Sciences Building, 24 Tyndall Avenue, Bristol, BS8 1TQ, UK

4 Co-first author

* correspondence : Sandrine.bonhomme@inra.fr (+33 1 30 83 32 89) and phills@sun.ac.za (+27 21 808 3066)

Summary (<200 words)

- Strigolactones are key hormonal regulators of flowering plant development and are widely distributed amongst streptophytes. In *Arabidopsis*, strigolactones signal via the F-box protein MORE AXILLARY GROWTH2 (MAX2), affecting multiple aspects of development including shoot branching, root architecture and drought tolerance. Previous characterization of a *Physcomitrella patens* moss mutant with defective

strigolactone synthesis supports an ancient role for strigolactones in land plants, but the origin and evolution of signaling pathway components is unknown.

- Here we investigate the function of a moss homolog of MAX2, PpMAX2, and characterize its role in strigolactone signaling pathway evolution by genetic analysis.
- We report that the moss *Ppmax2* mutant shows very distinct phenotypes from the moss SL-deficient mutant. In addition, the *Ppmax2* mutant remains sensitive to strigolactones, showing a clear transcriptional strigolactone response in dark conditions, and the response to red light is also altered. These data suggest divergent evolutionary trajectories for strigolactone signaling pathway evolution in mosses and vascular plants.
- In *P. patens*, the primary roles for MAX2 are in photomorphogenesis and moss early development rather than in strigolactone response, which may require other, still unidentified, factors.

Key words: Bryophyte, Moss, Hormone signaling, Strigolactone, Photomorphogenesis, F-box protein.

Introduction

Strigolactones (SLs) are plant hormones that were first identified as root-exudate products, exogenously indicating the vicinity of a host plant to parasitic plants such as *Striga* (Cook et al. 1966) and Arbuscular Mycorrhizal (AM) fungi (Akiyama et al. 2005). Roles for SLs in a range of endogenous developmental processes including shoot branching and root architecture were more recently described (Waldie et al. 2014; Lopez-Obando et al. 2015). SLs are present in most land plants (Xie et al. 2010) and the charophyte algal sister lineage to land plants

(Delaux et al. 2012), but signaling pathways are expanded in land plants relative to charophytes (Bowman et al. 2017). Therefore, SLs are key candidate facilitators for plant terrestrialization 480 million years (MY) ago (Bowman et al. 2017).

SL synthesis and signaling pathways have well characterized roles in branching in seed plants such as pea, *Arabidopsis*, *Petunia* and rice (Al-Babili and Bouwmeester 2015; Waters et al. 2017). Genes cloned from SL-deficient mutants have identified synthesis steps requiring a carotenoid isomerase DWARF27 (D27), two CAROTENOID CLEAVAGE DIOXYGENASES (CCD7 and CCD8), at least one Cytochrome P450 MORE AXILLARY GROWTH 1 (MAX1) (Al-Babili and Bouwmeester 2015), and the oxidoreductase-like enzyme LATERAL BRANCHING OXIDOREDUCTASE (LBO) (Brewer et al. 2016). In parallel, the study of SL-insensitive mutants has implicated several gene families in SL signaling. The first step of SL signaling is hormone perception, and this requires an α/β hydrolase enzyme, DECREASED APICAL DOMINANCE2/DWARF14/RAMOSUS3 (DAD2/D14/RMS3), that has been shown to interact with and cleave SL molecules *in vitro* (Hamiaux et al. 2012; Nakamura et al. 2013; de Saint Germain et al. 2016; Yao et al. 2016). *Petunia* DAD2 and rice D14 have been shown to interact in the presence of SLs with the F-box proteins MORE AXILLARY GROWTH 2A (PhMAX2A) and DWARF3 (D3), which are orthologous to *Arabidopsis* MAX2 (Hamiaux et al. 2012; Jiang et al. 2013; Zhou et al. 2013; Zhao et al. 2014). The current model for SL signaling mostly builds on studies of shoot branching in angiosperms, proposing that SL perception by D14/AtD14 induces the recognition of specific target proteins by an $SCF^{D3/MAX2}$ complex. This process leads to ubiquitination and proteasome-mediated degradation of targets in a similar process to processes described for other plant hormones including gibberellins (Lopez-Obando et al. 2015; Waters et al. 2017). Whilst roles for MAX2 in SL signaling were first described around 15 years ago (Stirnberg et al. 2002; Johnson et al. 2006; Stirnberg et al. 2007; Shen et al. 2012), the identification of DWARF53 (D53)/SUPPRESSOR OF MAX2-LIKE (SMXL) proteins as putative targets of the $SCF^{D3/MAX2}$ complex is more recent (Jiang et al. 2013; Stanga et al. 2013; Zhou et al. 2013; Soundappan et al. 2015; Wang et al. 2015).

Arabidopsis max2 mutants were also isolated in early genetic screens for delayed dark-induced senescence (Woo et al. 2001), and light hyposensitivity (Shen et al. 2007). Whereas the involvement of SLs in leaf senescence has been confirmed (Yamada et al. 2014; Ueda and Kusaba 2015), the photomorphogenesis phenotype of *max2* mutants appears independent of the SL pathway (Shen et al 2012). Furthermore, a requirement for MAX2 in other butenolide

signaling pathways was demonstrated by the isolation of *max2* mutants in a genetic screen for insensitivity to smoke-derived karrikins (Nelson et al. 2011; Waters et al. 2012). Karrikins induce *Arabidopsis* seed germination and affect seedling photomorphogenesis through a similar but distinct signaling pathway to SLs (Scaffidi et al. 2014; Waters et al. 2014), and an α/β hydrolase protein closely related to D14, KARRIKIN INSENSITIVE 2 (KAI2), is required for the response to karrikins (Waters et al. 2012). Whilst karrikins have not been detected in plants, KAI2 is the presumed receptor of an unknown plant-produced KAI2-ligand (KL) (Scaffidi et al. 2013; Waters and Smith 2013; Conn and Nelson 2015). Thus, the MAX2 F-box protein is involved in several signaling pathways apart from strigolactone signaling.

Although several components of the strigolactone synthesis and signaling pathways are shared amongst land plants, their roles in early diverging land plant lineages and contribution to plant evolution are unknown (Bowman et al. 2017). We addressed this evolutionary question using the moss *Physcomitrella patens* (*P. patens*) as a model representing an ancient divergence in land plant evolution. Whilst *CCD7* and *CCD8* orthologues are found in the *P. patens* genome, a true orthologue of *MAX1* is absent (Delaux et al. 2012). We previously generated *Ppccd8* SL-deficient mutants and demonstrated SL-functions in repressing radial plant growth and gametophore branching (Proust et al. 2011; Hoffmann et al. 2014; Coudert et al. 2015). Consideration of signaling pathways has revealed no true orthologue of the *D14* receptor gene, but there are 13 *PpKAI2-LIKE* genes that are closer to the *KAI2* α/β hydrolase clade in *P. patens* (Delaux et al. 2012; Lopez-Obando et al. 2016a). Phylogenetic analyses have also identified a single putative homologue for the F-box protein gene *MAX2* (Delaux et al. 2012) and three to four *PpSMXL* genes (Zhou et al. 2013).

Here we wished to explore SL signaling pathway evolution, and we focused on the role of the *P. patens MAX2* gene, testing whether *PpMAX2* is involved in the SL response. We also generated *PpMAX2* KO mutants and characterized their response to SL and red light at the phenotypic and molecular level. Our data indicate that similarly to MAX2 from *Arabidopsis*, *PpMAX2* is involved in photomorphogenesis. However, *PpMAX2* is probably not involved in generating a SL response.

Materials and Methods

P. patens **growth conditions**

The Gransden wild-type strain of *P. patens* was used and grown as previously described in a culture room at 24°C (day)/22°C (night) with a light regime of 16 h light/8 h darkness and a quantum irradiance of 80 µE m^{-2} s^{-1} (Proust et al. 2011; Lopez-Obando et al. 2016b). For phenotypic analysis, fragmented protonemal tissue was grown for 7 days on PP-NH_4 medium (=PP-NO_3 medium supplemented with 2.7 mM NH_4-tartrate) then transferred to PP-NO_3 medium (Ashton et al. 1979; Hoffmann et al. 2014). Sporogenesis was induced in Magenta vessels in which 21/28-day-old plants were grown on soil plugs (or PP-NO_3 medium) for 10 days as above and then transferred to a growth chamber at 15°C with 8 h of light per day and a quantum irradiance of 15 µE m^{-2} s^{-1} and rinsed once a week with sterile tap water till capsule maturity (after 2 to 3 months). For red light experiments, plants were grown on PP-NO_3 medium, at 24°C with a continuous red-light regime of 46 µE m^{-2} s^{-1}.

Generation of *Ppmax 2-1, Ppmax2-2* and *Ppccd8-Ppmax2* mutants

Moss protoplasts were obtained and transformed as described previously (Trouiller et al. 2006). For the *Ppmax2-1* mutant, a 735 bp *PpMAX2* genomic 3' CDS flanking sequence fragment was cloned in the pBHRF vector (Thelander et al. 2007), digested with *Nar*I and *Hpa*I. Next, an 886 bp *PpMAX2* genomic 5' CDS flanking sequence fragment was inserted into *Avr*II/*Xho*I sites of the pBHRF vector carrying the 3' CDS flanking sequence (PpMAX2-KO1 construct). For the *Ppmax2-2* mutant, a 1170 bp 5' CDS flanking sequence fragment and a 1170 bp 3' CDS flanking sequence fragment were amplified and subcloned into pJET1.2 vector (Fermentas) with a Geneticin/G418 resistance cassette from pMBL11a plasmid (Knight et al. 2002) (PpMAX2-KO2 construct). WT protoplasts were transformed with the PpMAX2-KO1 or the PpMAX2-KO2 constructs, and transformants were selected on 30 mg l^{-1} Hygromycin B or 50 mg l^{-1} G418, respectively. For the *Ppccd8-Ppmax2* double mutant, protoplasts from the single *Ppccd8* mutant were transformed with a construct carrying the same flanking sequences as PpMAX2-KO2, subcloned into the pJET1.2 vector, with a Hygromycin resistance cassette from pMBLH8a (Knight et al. 2002). Transformants were selected on 30 mg l^{-1} Hygromycin B. Stable transformants of the *PpMAX2* gene were confirmed by PCR using specific primers (Fig. S1 and Table S1).

Protoplast assays

Protoplasts were isolated as described in (Trouiller et al. 2006), counted, and kept overnight in the dark at 24°C, in liquid 8.5 % mannitol PP-NH_4. The next day, drops of 750 protoplasts gently mixed with 0.7% top agar (v/v) were transferred on 8.5 % mannitol PP-NH_4 plates,

with various (0 to 3 μM) concentrations of (±)-GR24 for 5 days, prior to transfer onto plates without mannitol (but with (±)-GR24).

Molecular cloning and subcellular protein localization

Generating the PPpMAX2:GUS lines

The *ZmUbi-1* promoter was eliminated from the pMP1300 vector [http://labs.biology.ucsd.edu/estelle/Moss_files/pMP1300-K108N+Ubi-GW-GUS.gb] by PCR amplification using primers Ubi-pr and Ubi-exp (Table S1) and the plasmid backbone was self-ligated and renamed pMP1301. A 1961 bp promoter region for *PpMAX2* was amplified from *P. patens* gDNA using primers PPpMAX2_F and PPpMAX2_R (Table S1). The product was purified and cloned into the vector pCR®8/GW/TOPO® (Life Technologies®, USA-CA). An LR-clonase reaction between the pMP1301 and pCR8::*PPpMAX2* plasmids yielded *PPpMAX2*:GUS, which was used to transform WT *P. patens*. A stable G418 resistant line was used for subsequent histochemical analysis to determine GUS localisation.

Generating the ZmUbi:gfp:PpMAX2 lines

Single-stranded *P. patens* cDNA was used as template to amplify the *PpMAX2* coding sequence using the PpMAX2_F and PpMAX2_R primer set (Table S1). The 2493 bp product was cloned into the pCR®8/GW/TOPO®. pCR8::PpMAX2 was recombined with the pMP1335 vector [http://labs.biology.ucsd.edu/estelle/Moss_files/ pK108N+Ubi-mGFP6-GW.gb] to get pMP1335::*PpMAX2*. pMP1335::*PpMAX2* was linearised by *Sfi*I digestion and transformed into WT *P. patens*. Stable G418 resistant lines were screened for insertion by PCR using the GFP_F and PpMAX2_R primers (Table S1). For one of these positive *GFP:PpMAX2* lines the localisation of the recombinant GFP:PpMAX2 was determined by visualising protonemal tissue on a confocal microscope (Carl Zeiss Confocal LSM 780 Elyra with SR- SIM superresolution plasform). For analysis, protonemal tissue was fixed in 4% (v/v) formaldehyde for 10 min and then stained with a 0.0125% (w/v) Hoescht33342 solution. Images were analysed by the ZEN 2012 (blue edition) software package (Carl Zeiss, Germany).

***Arabidopsis* complementation and phenotyping experiments**

Constructs in which the *PpMAX2* coding sequence was constitutively expressed alone or in a GFP fusion were introduced into the *max2-3* (N592836) T-DNA insertion mutant. The pUbi10 promoter, corresponding to the first 634 base pairs immediately upstream of the

ubiquitin-10 gene from Arabidopsis (At4g05320) was used to drive *PpMAX2* expression (Grefen et al. 2010). Expression of the *PpMAX2* mRNA and/or fluorescence of the GFP were checked in the corresponding transformed lines (Fig. S2). Results for two independent lines carrying each *PpMAX2* construct are shown. Hypocotyl length under low fluence experiments were carried out as previously described (de Saint Germain et al. 2016).

RNA extraction and gene expression analyses

Gene expression analyses were done by reverse-transcription quantitative PCR (RT-qPCR) as previously described (Hoffmann et al. 2014; Lopez-Obando et al. 2016a), with primers listed in Table S1.

Statistical analyses

For statistical analyses, ANOVA and Kruskal-Wallis tests were used (R Commander version 1.7-3).

Results

Physcomitrella patens contains a single *MAX2* homologue

The single *P. patens MAX2* homologue (Pp3c17_1180v3) was named *PpMAX2* (Delaux et al. 2012; Li et al. 2016). Phylogenetic analysis of full-length predicted MAX2 proteins indicated that, in contrast to previously published phylogenies that used a higher number of EST and full-length sequences, MAX2 from *P. patens*, *Marchantia polymorpha* and *Selaginella moellendorffii* formed a separate clade to seed plant proteins (Fig. S3a) (Delaux et al. 2012; Bythell-Douglas et al. 2017). Thus, the precise relationships between MAX2 homologues in vascular plants and those in non-vascular plants remain ambiguous. Nevertheless, the lack of any other close homologue in moss and the fact that *MAX2* is present as a single copy gene in a large majority of plant genomes suggest that *PpMAX2* is likely orthologous to *AtMAX2*. *PpMAX2* has no intron (Fig. S3b), and the predicted PpMAX2 protein is larger than vascular plant MAX2 proteins, containing C terminal insertions (Fig. S3c). Alignment of several predicted MAX2 protein sequences from vascular plants and bryophytes showed that PpMAX2 has a conserved F-box domain and similar LRR repeats composition to AtMAX2, with the exception that LRR13 is longer and consequently could not be modeled to existing F-box structures in this region (Fig. S3c-d).

PpMAX2 is expressed in most cells, and PpMAX2 localizes to the nucleus

To characterize the expression profile of *PpMAX2*, a 1961 bp promoter fragment was cloned upstream of the GUS coding sequence and introduced into the neutral Pp108 locus of wild-type (WT) moss plants by targeted insertion (Schaefer and Zryd 1997). Expression of the GUS reporter was observed in protonemal filaments, but not at the very tips of caulonema (Fig. 1a). Expression was also observed in gametophore axes and leaves (Fig. 1a-d), with stronger staining in older leaves than in young leaves at the top of the gametophore (Fig. 1c,d). This pattern was corroborated by expression data from the *P. patens* eFP-Browser and Genevestigator public databases (Hiss et al. 2014; Ortiz-Ramirez et al. 2016), that also indicated strong expression in sporophytes (Fig. S4). To determine the sub-cellular localization of PpMAX2, a GFP sequence was inserted in-frame and upstream of the PpMAX2 protein coding sequence, and introduced into WT plants. In accordance with knowledge of F-box protein function from flowering plants (Stirnberg et al. 2007), PpMAX2 localized to nuclei in protonemal cells (Fig. 1e-h).

Ppmax2 mutants are small plants with few but large gametophores, and show converse phenotypes to *Ppccd8* mutants

To determine the role of PpMAX2, *Ppmax2* mutants were engineered by targeted replacement using two replacement strategies, and two independent knockout lines were obtained (Fig. S1a,b). Whilst regeneration efficiencies were very low relative to WT plants (not shown), both *Ppmax2-1* and *Ppmax2-2* mutants showed the same phenotype (Fig. 2a) with very few protonema and rapid differentiation of large gametophores relative to WT plants (Fig. 2a). *Ppmax2* mutants were small with limited growth after several weeks of culture (Fig. 2b,c). When grown on soil plugs, plant diameter and the number of gametophores per plant were considerably reduced (Fig. 2c-d) and no sporophytes were found. We also tested the effect of the *Ppmax2* mutation on gametophore branch patterning (Coudert et al. 2015). Although the size of the apical inhibition zone (the apical portion of gametophores devoid of branches) was slightly smaller and the overall branch number was slightly higher in *Ppmax2-1* mutants than in WT plants, the spacing between branches was similar in both genotypes (Fig. 2e, Fig S5). These data suggest that *PpMAX2* plays a minor role in gametophore branching. If *PpMAX2* has roles in moss SL signaling, we would expect that the phenotype of *Ppmax2* mutants should resemble *Ppccd8* SL biosynthesis mutant phenotype, as in flowering plants (Gomez-Roldan et al. 2008; Umehara et al. 2008). However, *Ppmax2* and *Ppccd8* appear to have

opposite phenotypes, as if *Ppmax2* displayed SL over-production or a constitutive SL response (Fig. 2a,b,d).

Ppmax2 mutants can elicit a strigolactone response

As SL molecules are very difficult to quantify, we used an indirect approach to determine whether *Ppmax2* overproduces SL and quantified expression of *PpCCD7*, a SL-responsive gene whose transcript levels decrease following (±)-GR24 application (Proust et al. 2011). We used *Ppccd8* mutant plants for these experiments as the SL response is easier to observe in mutants than in WT plants (Hoffmann et al. 2014), and plants were transferred onto media containing no exudate, 1 µM (±)-GR24, WT, *Ppccd8* or *Ppmax2-1* exudate. *PpCCD7* transcript levels were assayed 6 h after transfer (Fig. 3). Transfer of plants onto medium containing *Ppccd8* exudate led to *PpCCD7* transcript levels similar to those observed following transfer onto fresh medium. However, transfer onto medium containing *Ppmax2-1* exudate led to a significant decrease of *PpCCD7* transcript level, as was observed following transfer onto media containing (±)-GR24 or WT exudate (Fig. 3). Thus *Ppmax2-1* exudate affects *PpCCD7* transcript levels in a similar way to WT exudate, and *Ppmax2-1* is likely to produce SL at similar levels to WT plants.

Ppmax2 mutants show growth responses to (±)-GR24 application

The response of *Ppmax2* mutants to exogenously applied (±)-GR24 was tested and compared to the response of *Ppccd8* mutants to identify any roles for PpMAX2 in SL signaling. These experiments were carried out using dark-grown caulonema where differences in growth are most pronounced (Hoffmann et al. 2014), and plants were grown vertically so that caulonema extending with a negative gravitropism on the medium could be directly measured. Under these conditions both *Ppmax2-1* and *Ppccd8* mutant caulonema showed significant and dose-dependent growth suppression (Fig. 4a). The relative decrease in caulonema length was greater in the *Ppmax2-1* mutant than in *Ppccd8* in all tested conditions (Fig. 4a). We also assayed SL responsiveness using a protoplast regeneration assay, and found that fewer plants regenerated in WT and *Ppccd8* and *Ppmax2* mutant plants following (±)-GR24 application, with the response being dose-dependent (Fig. 4b). Thus, *Ppmax2* mutants can respond to SL application, and the response is pronounced in caulonema when mutants are grown in the dark, or in protoplasts regenerating in the light.

310

311 ***Ppmax2* mutants show transcriptional responses to (±)-GR24 application**

312 *Ppmax2* responses to SL were further analyzed using SL-responsive genes as molecular
313 markers. The *PpCCD7* transcript level was very low in *Ppmax2-1* mutants relative to levels in
314 *Ppccd8* mutants and WT plants, and in contrast to a significant response observed in WT and
315 *Ppccd8,* no significant decrease was noted in *Ppmax2-1* mutants 6 h after transfer on medium
316 with (±)-GR24, (Fig. 4c). We also measured transcript abundance of the *PpKUF1LA* gene
317 (Pp3c2_34130v3.1), a moss homologue of *Arabidopsis KAR-UP F-BOX1* (*KUF1*). *KUF1*
318 transcript levels are sensitive to (±)-GR24 application in *Arabidopsis* SL biosynthesis mutants
319 (Nelson et al. 2011; Waters et al. 2012; Stanga et al. 2016). *PpKUF1LA* (Pp3c2_34130v3.1)
320 transcript levels increased 6 h after transfer on medium containing (±)-GR24 in both light-
321 grown WT and *Ppccd8* mutants, but no response was detected in light-grown *Ppmax2-1*
322 mutants (Fig. S6a). As the bioassay suggested a *Ppmax2-1* response to SL in the dark (Fig.
323 4a), we tested gene expression in dark grown plants. In contrast to WT and *Ppccd8* mutant
324 plants, no decrease of the *PpCCD7* transcript level was observed in *Ppmax2* mutants
325 following transfer on (±)-GR24 (Fig. S6b). However, in dark-grown *Ppmax2-1* plants,
326 transcript levels of *PpKUF1LA* significantly increased following transfer on (±)-GR24 as in
327 WT and *Ppccd8* mutant plants (Fig. 4d). Thus *Ppmax2* mutants remain responsive to
328 exogenously-applied SL.

329

330 ***PpMAX2* expression is light responsive, and *Ppmax2* has impaired light responses**

331 To further investigate roles for *PpMAX2* in light-regulated development, WT tissues were
332 grown in the light for 7 days and then placed in the dark for 5 days prior to transfer into red
333 light for increasing lengths of time. *PpMAX2* transcript levels were higher in the dark than in
334 the light (Fig. 5a). One hour of red light treatment led to a significant decrease in *PpMAX2*
335 transcript levels, and a 3-hour treatment resulted in a minimal expression level that was
336 comparable to *PpMAX2* expression levels in white light (Fig. 5a), thus *PpMAX2* expression is
337 light regulated. In white light, gametophores with the same number of leaves as WT, *Ppccd8*
338 or *Ppmax2-2* mutant plants were taller in *Ppmax2-2* mutants (Fig. 5b), showing an etiolation
339 phenotype associated with light regulated development in other plants. To investigate a
340 potential role for *PpMAX2* in photomorphogenesis, *Ppmax2-1* mutants were grown under
341 continuous red light for 25 days. A strong etiolation phenotype was observed in *Ppmax2-1*
342 mutant gametophores but not in WT or *Ppccd8* (Fig. 5c). We analyzed the transcript levels of

genetic markers for light response in WT versus *Ppmax2-1* mutant tissues. *Ppmax2-1* mutant and WT plants were first grown in white light for 2 weeks and then transferred into the dark for 4 days prior to exposure to red light for increasing time periods (0.5h to 24h). After red light treatment, transcript levels of both *ELONGATED HYPOCOTYL 5a* (*PpHY5a*) and *NADPH-PROTOCHLOROPHYLLIDE OXIDOREDUCTASE 1* (*PpPOR1*) were measured by RT-qPCR (Fig. 5d,e). The transcript levels of *PpHY5a* showed a transient and rapid increase with red light exposure in WT whilst remaining almost unchanged in *Ppmax2-1*. *PpPOR1* transcript levels also increased with red light exposure in WT but remained lower in *Ppmax2-1*. The *Ppmax2* mutants thus have an impaired response to red light.

Ppmax2 is epistatic to _Ppccd8_

To examine the genetic interaction between *PpMAX2* and *PpCCD8*, *Ppmax2* mutants were engineered in the *Ppccd8* mutant background (Fig. S1c). *Ppccd8-Ppmax2* double mutants had a phenotype similar to that of *Ppmax2* mutants, with no additive effects on plant extension or gametophore development, indicating that the *Ppmax2* mutation can override the effect of the *Ppccd8* mutation (Fig. 6a,b). Whilst up-regulated *PpCCD7* transcript levels are a genetic marker of *Ppccd8* mutants, *PpCCD7* expression was down-regulated in both *Ppmax2-1* and *Ppccd8-Ppmax2* double mutants (Fig. 6c), further suggesting that the *Ppmax2* mutation is epistatic to the *Ppccd8* (Fig. 6a,b).

PpMAX2 cannot complement _Atmax2_ mutant phenotypes

The data above suggest that roles for MAX2 in SL signaling are not conserved between *P. patens* and *Arabidopsis*. To test this hypothesis, we heterologously expressed *PpMAX2* in the *Atmax2-3* mutant background, and used *AtMAX2* as a control (Fig. 7, FigS2). Whilst *AtMAX2* expression was able to restore WT plant phenotypes, *PpMAX2* expression failed to complement the reduced height, higher branching and elongated hypocotyl under low fluence mutant phenotypes of *Atmax2-3* (Fig. 7). Some partial complementation of the branching phenotype was observed in the lines where the *PpMAX2* gene was fused to the GFP, with intermediate branching between WT and *Atmax2-3* (Fig. 7c). However, as these lines are smaller in size than the *Atmax2-3* mutant (Fig. 7a), one cannot conclude that these were complemented lines. Thus *PpMAX2* and *AtMAX2* are not functionally equivalent.

Discussion

Phylogenetic studies have suggested that SL biosynthesis and signaling pathways are conserved amongst land plants (Proust et al. 2011; Delaux et al. 2012; Waters et al. 2012; Bowman et al. 2017). SLs or SL-like compounds are found in bryophytes and in the moss, *P. patens*, both the PpCCD7 and PpCCD8 proteins have been shown to have *in vitro* enzymatic activities that are conserved with seed plants, indicating probable conservation of at least the early steps in SL biosynthesis (Decker et al. 2017). Homologues of key genes of the SL signaling pathway are found in the *P. patens* genome, with one *PpMAX2*, 13 *PpKAI2-LIKE* and four *PpSMXL* genes. Whilst it is likely that some of the KAI2 proteins may function as SL receptors in moss (Lopez-Obando et al. 2016a), as yet no functional studies demonstrate their involvement in SL perception. This study focused on the moss *PpMAX2* gene and our results indicate that roles in photomorphogenesis are conserved with *Arabidopsis* MAX2, but that a role of PpMAX2 in SL signaling is unlikely.

SL signaling pathway in moss is distinct from flowering plants, and does not require the PpMAX2 F-box protein

The *Ppmax2* phenotype and the ability of the mutant to respond to SL are evidence that PpMAX2 is not necessary for SL signaling. Gametophore branching (Coudert et al. 2015) and plant spread phenotypes are different between the *Ppccd8* and *Ppmax2* mutants. These results contrast with mutant phenotypes in seed plants, where shoot branching and plant height are comparable in *ccd8* and *max2* mutants (Gomez-Roldan et al. 2008; Umehara et al. 2008). In *Arabidopsis*, the *max2* mutation is considerably more pleiotropic in comparison to the *ccd8* (*max4*) mutation. SL-independent seed germination and photomorphogenesis phenotypes are observed in *Atmax2* mutants (Nelson et al. 2011; Shen et al. 2012). As both SL and the unidentified KAI2-Ligand (KL) signal through AtMAX2, the mutant combines the effect of alteration of several pathways. It is possible that in moss the *Ppmax2* mutation is also highly pleiotropic and that the strong effect of the *Ppmax2* mutation masks or overrides the *Ppccd8* phenotype. This hypothesis is supported by the *Ppccd8-Ppmax2* double mutant phenotype that resembles the *Ppmax2* phenotype.

Several bioassays were used to test the SL response of the *Ppmax2* mutant, and the *Ppmax2* mutant is sensitive to (±)-GR24 applications under protoplast regeneration and early growth in light conditions, as well as during caulonemal growth in the dark. Furthermore, a

transcriptional response of SL-responsive genes in the *Ppmax2* mutant is observed in dark conditions. We observed that the scale of the *Ppmax2* response to (±)-GR24 was variable compared to that of WT or *Ppccd8* mutants (Fig. 4). This may be related to the use of racemic (±)-GR24 that could induce SL-independent effects (Scaffidi et al. 2014), not yet characterized in moss. The fact that PpMAX2 expression does not restore the *Arabidopsis max2* phenotypes also argues against a role in SL response, although the moss PpMAX2 F-box protein may not be able to recognize *Arabidopsis* protein interaction partners in transformed lines due to differences in C-terminus protein structure (Fig. S3,c).

Our conclusion that PpMAX2 is not crucial for SL signaling in moss leads us to hypothesize that other factors (e.g. F-box proteins) may be required. Interestingly, MAX2-independent SL responses have previously been hypothesized for roots of seed plants (Ruyter-Spira et al. 2011; Shinohara et al. 2013; Walton et al. 2016) and high doses of (±)-GR24 (5-10 μM) can induce a response in *Arabidopsis max2* mutants (Ruyter-Spira et al. 2011). Furthermore, MAX2-independent promotion of stromule formation can be induced by (±)-GR24 (Vismans and van der Meer 2016). An unknown factor involved in SL signaling could thus be conserved between moss and vascular plants and able to signal with more subtle effects than the MAX2 pathway. SL signaling in moss could also be F-box protein independent, implicating different downstream mechanisms to those so far described in vascular plants in signaling. Investigation of the roles of *PpSMXL* genes, and putative degradation of PpSMXL proteins should clarify this point in the future.

Do *Ppmax2* and *Ppccd8* mutants really have opposite phenotypes?

The response to SL of the *Ppmax2* mutant was difficult to pinpoint because *Ppmax2* mutants have a converse phenotype to *Ppccd8* mutants. Whilst *Ppmax2* mutant plants are small and have few protonemal filaments, *Ppccd8* plants produce many protonemata and spread across the substrate. We previously showed that whilst WT plants cease protonemal spread in response to near neighbors, *Ppccd8* mutants are insensitive to neighbors in Petri cultures (Proust et al. 2011). This phenomenon leads to small plant size as in the *Ppmax2* mutants and WT plants grown on high (non-physiological) doses of (±)-GR24 are also small with comparable size to *Ppmax2* plants (Fig. S7). Another line of evidence supporting the interpretation that *Ppmax2* and *Ppccd8* mutant phenotypes are converse is the transcript level of several SL-responsive genes, conversely affected in *Ppccd8* and *Ppmax2* mutants. For

instance, *PpCCD7* transcript levels are very low in *Ppmax2* but much higher in *Ppccd8* mutants (Fig. 4c).

If the phenotypes of *Ppccd8* and *Ppmax2* mutants are converse, *Ppmax2* plants may over-produce and/or over-accumulate SLs. This hypothesis was tested indirectly by monitoring the *Ppccd8* mutant response to *Ppmax2* exudate versus *Ppccd8* or WT exudates or (±)-GR24 treatment (Fig. 3), and the results suggest that *Ppmax2* does not over-produce SLs, but verification by SL quantification is required, and these assays are challenging in moss. Alternatively, *Ppmax2* mutants could phenocopy a constitutive SL response.

As PpMAX2 is an F-box protein, putatively involved in degradation processes by the proteasome system, PpMAX2 could target activators of SL signaling for degradation, and such activators so far remain unidentified. SMXL proteins are known targets for degradation in seed plant SL signaling pathways, and SMXLs are considered as repressors of this pathway (Soundappan et al. 2015; Wang et al. 2015). Interestingly, the converse phenotypes of *Ppmax2* and *Ppccd8* mutants did not hold for gametophore branching, as *Ppmax2* gametophores did not lack branches as in a pea *CCD8* overexpressor line (*PpRMS1OE*) (Coudert et al. 2015). PpMAX2 may function in protonema and early gametophore development, but not in later development (Fig. 8).

The low levels of *PpCCD7* expression in *Ppmax2* in comparison to WT suggest that PpMAX2 and SL are not completely independent. However, this could be an indirect effect of reduced gametophore production in the mutant (Fig. 2d) as the highest *PpCCD7* transcript levels were observed at the base of the gametophore (Proust et al. 2011). There may also be indirect feedback control on transcript levels. In vascular plants, environmental conditions (N, P, drought) or endogenous factors as auxin control the expression levels of SL biosynthesis genes (Al-Babili and Bouwmeester 2015; Ligerot et al. 2017). It would be interesting to quantify auxin levels in both *Ppmax2* and *Ppccd8* mutants to test whether differences in IAA levels translate into differences in *PpCCD7* transcript levels. Further experiments are needed to have a clear understanding of the moss SL signaling pathway. In particular, biochemistry to test protein interactions and quantification of the levels of other hormones should be very informative.

The role of MAX2 in light response is similar between moss and seed plants

The shoot elongation phenotype of the *Ppmax2* mutant under red light and its misregulation of light responsive genes support the notion that *PpMAX2* plays a role in light responses (Fig. 5), as does its flowering plant homologue (Shen et al. 2007). The paucity of caulonemal filaments in *Ppmax2* may also be related to a defective light response as a similar phenotype was observed in the light sensing-defective *P. patens Δhy5ab* and *pubs-hy2* double mutants (Yamawaki et al. 2011; Chen et al. 2012). In our experiments, tissue used for RNA extraction included a mix of protonemata and gametophores, and the ratio of different tissue types may be different in mutants versus WT plants given their distinct phenotypes. Whilst we interpret the light responsive gene expression data with caution, our results suggest that the ancestral role of MAX2 may be to promote photomorphogenesis. Despite this likely shared role with AtMAX2, PpMAX2 cannot complement the *Atmax2* mutant hypocotyl phenotype under low fluence light (Fig. 7d), potentially because *Arabidopsis* MAX2 and moss PpMAX2 protein partners may not recognize one another. As with the shade avoidance response of vascular plants it is possible that PpMAX2 helps plants to grow in an ideal amount of light. In this instance, PpMAX2 could allow plants to respond to low light, delaying gametophore growth and investing energy in spreading protonemal tissues to find light patches. This regulation could also require HY5, given the similar phenotypes of the mutants (see above) and the misregulation of *HY5a* transcript levels in the *Ppmax2* mutant.

An ancestral role of MAX2 in moss development

Our data and our model for roles for MAX2 in land plants (Fig. 8) open the question of an evolutionary benefit to seed plants in recruiting this F-box protein to SL signaling. We propose that combining the ability of MAX2 to regulate the levels of downstream proteins (e.g. SMXL proteins) would have added a level of fine (endogenous) regulation to photomorphogenesis or aspects of development already under the control of this F-box protein in early land plants. Further studies in other land plants including gymnosperms, lycophytes and other bryophytes will answer this question.

The expression of the *PpMAX2* gene during all stages of moss development is in agreement with the putative function of PpMAX2 as a component of an SCF complex regulating the homeostasis of multiple targets. Phenotypes of *Ppmax2* mutants and the *Ppccd8-Ppmax2* double mutant indicate an early and simultaneous role in repressing gametophore/bud differentiation and stimulating the chloronema to caulonema transition. Thus PpMAX2 could act conversely to SLs which repress plant spread (Proust et al. 2011). Interestingly, in moss,

auxin has been shown to regulate the chloronema to caulonema transition (Ashton et al. 1979; Prigge et al. 2010; Jang and Dolan 2011), while cytokinins induce bud differentiation (von Schwartzenberg et al. 2007). It would thus be interesting to investigate both the auxin and cytokinin status of the *Ppmax2* mutant. Involvement of all three hormonal pathways in moss gametophore branching has been recently addressed (Coudert et al. 2015), and this study suggests that auxin, cytokinin and SL signaling may interact, as in vascular plants.

In seed plants, MAX2 has been linked to signaling by a still unknown KL compound "which interacts at some level with auxin and light signaling to regulate growth and development" (Waters and Smith 2013; Conn and Nelson 2015). As the receptor KAI2 is ancestral, this pathway may be present in bryophytes. It could then be argued that the *Ppmax2* phenotype is the consequence of disturbing this second signaling pathway (Fig. 8). Given this scenario, KL signaling could interfere with or mask SL signaling, because the phenotype of the *Ppccd8-Ppmax2* double mutant is closer to that of *Ppmax2*. It has not yet been possible to test this hypothesis as moss does not seem to respond to karrikins (Hoffmann et al. 2014) and the nature of KL compound is still elusive. The study of interactions of PpMAX2 with some of the 13 PpKAI2-LIKE and/or the four PpSMXL putative targets found in moss genome (Bennett and Leyser 2014; Lopez-Obando et al. 2016a) will be key to confirming the place of PpMAX2 in these signaling events.

Acknowledgements: We thank Sonia Canessane for *Arabidopsis* transformants selection and first characterization, François Didier-Boyer for the generous supply of (±)-GR24, Michel Burtin and Jean-Paul Saint-Drenan for the technical assistance in red light experiments. PH, JK and RdV thank Shaun Peters for valuable discussions and insights.

Author contributions

CR, SB, ML-O, JK, RdV, PH, JH and YC designed the research. BH, LM, ML-O, YC, ASG, PH, RdV and SB conducted experiments, SB, ML-O, PH, JH, YC and CR analyzed data and wrote the article with contribution of all authors.

Funding: This research was supported by the Agence Nationale de la Recherche (contract ANR-12-BSV6-004-01), by the BBSRC (BB/L00224811) and Gatsby (GAT2962), and by the National Research Foundation (SARChi Research Chair "Genetic tailoring of biopolymers") of South Africa. The IJPB benefits from the support of the Labex Saclay Plant Sciences-SPS (ANR-10-LABX-0040-SPS). This article is based upon work from COST Action FA1206 STREAM, supported by COST (European Cooperation in Science and Technology). YC thanks the CNRS ATIP-Avenir programme for ongoing support.

Figure legends:

Fig. 1: Pattern of *Physcomitrella patens PpMAX2* gene expression and subcellular localization of the protein. (a-d): Pattern of *PpMAX2* gene expression by staining of a moss line expressing the GUS coding sequence under the control of *PpMAX2* gene promoter (inserted in Pp108 locus) (a) protonema cells, (b-d) gametophore leaves and stems; arrow in (c): rhizoids. scale bars: (a-b): 0.1 mm; (c): 1 mm (d): 0.5 mm. (e-h) Nuclear localization of PpMAX2 in a protonemal tip cell of a WT moss line transformed with a mGFP6::PpMAX2 translational fusion by homologous recombination. (e) Nucleus labeling with Hoescht33342. (f) GFP fluorescence (g) chloroplast autofluorescence (h) Merge of all 3 images (e-g), indicating co-localization of Hoescht33342 and GFP to the nucleus. Scale bar: 20 μm.

Fig. 2: *Physcomitrella patens Ppmax2* mutants are affected in development and show contrasting phenotype to the *Ppccd8* SL synthesis mutant. (a): Bright field photographs of 7 day-old (left), 13 day-old (middle) and 20 day-old plants (right). Scale = 500 μM (b): Comparison of *Ppmax2* mutants plant diameter to that of WT and *Ppccd8* mutant after 5 weeks (left, mean ± SE of 3 plates with 16 plants measured per plate) and 5 month (right, mean ± SE of 10 plants grown on soil plugs) growth in the light. Asterisks denote significant differences between WT and mutants based on a Kruskal–Wallis test ($P < 0.001$) (c) Pictures of 5 month-old WT and *Ppmax2-1* plants grown on soil plugs. (d): Comparison of *Ppmax2-1* mutant fitness to that of WT and *Ppccd8* mutant in 5 month-old plants, measuring gametophore number per plant (left) and sporangia number per plant (right). Data are means of 10 plants ± SE. Asterisks denote significant differences between the genotypes based on a Kruskal–Wallis test (**$P<0.01$; ***$P<0.001$) (e): *Ppmax2-1* gametophore branching pattern

567 compared to that of WT (left panel). Apical inhibition zone size (middle panel) was reduced
568 in *Ppmax2-1* (mean ± SD; bilateral t-test different from WT,*p < 0.05), while distance to
569 closest branch was similar (mean ± SD).

570

571 Fig. 3: The *Physcomitrella patens Ppmax2* mutant exudate tested on *PpCCD7* expression is
572 similar to WT

573 Three-week-old *Ppccd8* plants were transferred for 6h on medium with 0μM (±)-GR24 (Ctl),
574 or 1μM (±)-GR24, or on medium where the WT, or the different mutants had grown (and
575 exuded SLs) for 3 weeks noted as "exud". Data represent means of transcript levels of 3
576 biological repeats relative to *PpAPT* expression level, ± SE. Different letters indicate
577 significantly different results based on a post-hoc Kruskal–Wallis test (P < 0.05).

578

579 Fig. 4: The *Physcomitrella patens Ppmax2* mutant is sensitive to the synthetic SL (±)-GR24.
580 (a) Caulonema length measurements in the dark in *Ppmax2-1* mutant and *Ppccd8* SL
581 synthesis mutant, following application of increasing concentrations of (±)-GR24. Control
582 (Ctl): same amount of acetone. Asterisks denote significant differences between the control
583 and the treatment within the genotypes based on a Kruskal–Wallis test (P < 0.001). (b)
584 Protoplast regeneration tests. Asterisks denote significant differences between the control and
585 the treatment within the genotypes based on a Kruskal–Wallis test (P < 0.001). (c) Transcript
586 levels of the SL responsive gene *PpCCD7* relative to *PpAPT* and *PpACT3* transcript levels in
587 WT, *Ppccd8* and *Ppmax2-1* grown for 3 weeks in the light. (d) Transcript levels analysis of
588 the SL responsive gene *PpKUF1LA* relative to *PpAPT* and *PpACT3* transcript levels in WT,
589 *Ppccd8* and *Ppmax2-1* mutants, grown for two weeks in the light then one week in the dark
590 and transferred onto control medium (Ctl) or 3 μM of (±)-GR24. On the right, a close-up of
591 transcript levels in *Ppmax2-1* is shown. Different letters indicate significantly different results
592 between non-treated genotypes based on a Kruskal–Wallis test (P < 0.05). Asterisks denote
593 significant differences between treated and control plants within a genotype based on a *post-*
594 *hoc* Kruskal–Wallis test (P < 0.001). Data represent means of 3 biological repeats, relative to
595 mean (*PpAPT-PpACT3*) transcript level ± SE.

596

597 Fig. 5: The *Physcomitrella patens Ppmax2* mutant has impaired photomorphogenesis. (a)
598 Transcript levels of *PpMAX2* gene in WT, following growth in the dark (5 days) then in red

599 light for increasing lengths of time (0.5h to 24h). Controls: growth in dark or light conditions
600 (6 days). Data represent mean of transcript levels of 3 biological repeats, relative to *PpACT3*
601 and *PpAPT* expression level, ± SE. Asterisks denote significant differences between the dark
602 control and the treatment based on a Kruskal–Wallis test ($P < 0.001$). (b) Leaf distribution on
603 gametophores from WT (blue dots) *Ppccd8* (orange squares) and *Ppmax2-2* (black triangles).
604 (c) Gametophore height of WT, *Ppccd8*, *Ppmax2-1* phenotype after 25 days under red light
605 (left, scale = 5 mm) and quantifications (right) mean of 3 Magenta, n=43-50 counted
606 gametophores per Magenta. Different letters indicate significantly different results between
607 genotypes based on a *post hoc* Kruskal–Wallis test. (d-e) Transcript levels of red light
608 response markers (*PpHY5* (d) and *PpPOR1* (e)), in WT and *Ppmax2-1* mutants following
609 different times of red light exposure as indicated below the histograms. WL= White Light
610 control. Data represent mean of transcript levels of 3 biological repeats, relative to *PpACT3*
611 expression level, ± SE. Asterisks denote significant differences between the genotypes based
612 on a Kruskal–Wallis test ($P < 0.001$).

613

614 Fig. 6 The *Physcomitrella patens Ppmax2* mutation is epistatic to *Ppccd8*. (a) Bright field
615 photographs of WT, single *Ppccd8*, single *Ppmax2* mutant and *Ppccd8-Ppmax2* double
616 mutant. Scale: left, 20 day-old: 1mm; right, 2 month-old: 5mm. (b) Comparison of *Ppccd8-*
617 *Ppmax2* mutant plant diameter to that of WT and *Ppccd8* and *Ppmax2* mutants after 4 weeks
618 (mean of 3 plates with 16 plants measured per plate, ± SE). Different letters indicate
619 significantly different results between genotypes based on an ANOVA ($P < 0.05$) (c)
620 Expression of the SL responsive gene *PpCCD7* relative to *PpAPT* and *PpACT3* expression in
621 *Ppccd8, Ppmax2-1* and *Ppccd8-Ppmax2* grown for 3 weeks in the light. Asterisks denote
622 significant differences between *Ppccd8* and the other mutants based on a *post-hoc* Kruskal–
623 Wallis test ($P < 0.001$). Data represent means of 3 biological repeats ± SE.

624

625 Fig.7: Expression of *Physcomitrella patens PpMAX2* gene in the *Arabidopsis max2* mutant
626 does not restore MAX2 function (a) Mean height and (c) mean number of rosette branches , ±
627 SE, from 4-week-old *Arabidopsis* plants (n=12) of each genotype 10 days after decapitation.
628 (b) Corresponding pictures of one exemplary plant per genotype are shown. (d) Hypocotyl
629 length of 5-day-old *Arabidopsis* plantlets (n=15) grown in vitro under low light intensity (20-
630 30 μE**)**. Names of the transformed plants indicate the construct harbored. Controls used for all
631 experiments were *Arabidopsis* WT Columbia (Col-0, white bar), *Atmax2-3* mutant (N592836,

632 black bar) and *Atmax2-3* transformed with constructs expressing *AtMAX2* under the control of
633 the pUbi10 promoter. Different letters indicate significantly different results based on a post-
634 hoc Kruskal–Wallis test ($P < 0.05$). Data represent means ± SE.

635

636 Fig. 8: Model for MORE AXILLARY GROWTH2 (MAX2) roles in land plants. In vascular
637 plants, the MAX2 F-box protein is central for shoot branching, seed germination and
638 photomorphogenesis, by mediating Strigolactone (SL), the still unknown KAI2 Ligand (KL)
639 and light signals. D14 and KAI2 are known receptors for SL and KL respectively. In moss,
640 the F-box protein, PpMAX2, is likely involved in photomorphogenesis and plant spread
641 (protonemal growth), but another F-box protein may be required for SL signaling. Receptors
642 for these signals are still to be identified among the numerous moss PpKAI2Like predicted
643 proteins. The similar photomorphogenic phenotypes of *Atkai2* and *Atmax2* mutants suggest
644 that the effect of light on development through MAX2 could, at least in part, be mediated via
645 changes in KL that are perceived by KAI2 (dotted line). Arrows on the left mean signaling
646 mediation. Arrows on the right mean positive action while blunt-ended lines mean repression.

647

648

649

650 ## References

651

652 Akiyama K, Matsuzaki K, Hayashi H (2005) Plant sesquiterpenes induce hyphal
653 branching in arbuscular mycorrhizal fungi. Nature 435 (7043):824-827
654 Al-Babili S, Bouwmeester HJ (2015) Strigolactones, a novel carotenoid-derived plant
655 hormone. Annu Rev Plant Biol 66:161-186. doi:10.1146/annurev-arplant-
656 043014-114759
657 Ashton NW, Grimsley NH, Cove DJ (1979) Analysis of gametophytic development in the
658 moss, *Physcomitrella patens* , using auxin and cytokinin resistant mutants. Planta
659 144 (5):427-435. doi:10.1007/bf00380118
660 Bennett T, Leyser O (2014) Strigolactone signalling: standing on the shoulders of
661 DWARFs. Curr Opin Plant Biol 22:7-13. doi:10.1016/j.pbi.2014.08.001
662 Bowman JL, Kohchi T, Yamato KT, Jenkins J, Shu S, Ishizaki K, Yamaoka S, Nishihama R,
663 Nakamura Y, Berger F, Adam C, Aki SS, Althoff F, Araki T, Arteaga-Vazquez MA,
664 Balasubrmanian S, Barry K, Bauer D, Boehm CR, Briginshaw L, Caballero-Perez J,
665 Catarino B, Chen F, Chiyoda S, Chovatia M, Davies KM, Delmans M, Demura T,
666 Dierschke T, Dolan L, Dorantes-Acosta AE, Eklund DM, Florent SN, Flores-
667 Sandoval E, Fujiyama A, Fukuzawa H, Galik B, Grimanelli D, Grimwood J,
668 Grossniklaus U, Hamada T, Haseloff J, Hetherington AJ, Higo A, Hirakawa Y,
669 Hundley HN, Ikeda Y, Inoue K, Inoue SI, Ishida S, Jia Q, Kakita M, Kanazawa T,

Kawai Y, Kawashima T, Kennedy M, Kinose K, Kinoshita T, Kohara Y, Koide E, Komatsu K, Kopischke S, Kubo M, Kyozuka J, Lagercrantz U, Lin SS, Lindquist E, Lipzen AM, Lu CW, De Luna E, Martienssen RA, Minamino N, Mizutani M, Mizutani M, Mochizuki N, Monte I, Mosher R, Nagasaki H, Nakagami H, Naramoto S, Nishitani K, Ohtani M, Okamoto T, Okumura M, Phillips J, Pollak B, Reinders A, Rovekamp M, Sano R, Sawa S, Schmid MW, Shirakawa M, Solano R, Spunde A, Suetsugu N, Sugano S, Sugiyama A, Sun R, Suzuki Y, Takenaka M, Takezawa D, Tomogane H, Tsuzuki M, Ueda T, Umeda M, Ward JM, Watanabe Y, Yazaki K, Yokoyama R, Yoshitake Y, Yotsui I, Zachgo S, Schmutz J (2017) Insights into Land Plant Evolution Garnered from the *Marchantia polymorpha* Genome. Cell 171 (2):287-304.e215. doi:10.1016/j.cell.2017.09.030

Brewer PB, Yoneyama K, Filardo F, Meyers E, Scaffidi A, Frickey T, Akiyama K, Seto Y, Dun EA, Cremer JE, Kerr SC, Waters MT, Flematti GR, Mason MG, Weiller G, Yamaguchi S, Nomura T, Smith SM, Yoneyama K, Beveridge CA (2016) *LATERAL BRANCHING OXIDOREDUCTASE* acts in the final stages of strigolactone biosynthesis in Arabidopsis. Proc Natl Acad Sci U S A 113 (22):6301-6306. doi:10.1073/pnas.1601729113

Bythell-Douglas R, Rothfels CJ, Stevenson DWD, Graham SW, Wong GK, Nelson DC, Bennett T (2017) Evolution of strigolactone receptors by gradual neo-functionalization of KAI2 paralogues. BMC biology 15 (1):52. doi:10.1186/s12915-017-0397-z

Chen YR, Su YS, Tu SL (2012) Distinct phytochrome actions in nonvascular plants revealed by targeted inactivation of phytobilin biosynthesis. Proc Natl Acad Sci U S A 109 (21):8310-8315. doi:10.1073/pnas.1201744109

Conn CE, Nelson DC (2015) Evidence that KARRIKIN-INSENSITIVE2 (KAI2) Receptors may Perceive an Unknown Signal that is not Karrikin or Strigolactone. Front Plant Sci 6:1219. doi:10.3389/fpls.2015.01219

Cook CE, Whichard LP, Turner B, Wall ME, Egley GH (1966) Germination of Witchweed (*Striga lutea Lour.*): Isolation and Properties of a Potent Stimulant. Science 154 (3753):1189-1190

Coudert Y, Palubicki W, Ljung K, Novak O, Leyser O, Harrison CJ (2015) Three ancient hormonal cues co-ordinate shoot branching in a moss. Elife 4. doi:10.7554/eLife.06808

de Saint Germain A, Clave G, Badet-Denisot MA, Pillot JP, Cornu D, Le Caer JP, Burger M, Pelissier F, Retailleau P, Turnbull C, Bonhomme S, Chory J, Rameau C, Boyer FD (2016) An histidine covalent receptor and butenolide complex mediates strigolactone perception. Nat Chem Biol 12 (10):787-794. doi:10.1038/nchembio.2147

Decker EL, Alder A, Hunn S, Ferguson J, Lehtonen MT, Scheler B, Kerres KL, Wiedemann G, Safavi-Rizi V, Nordzieke S, Balakrishna A, Baz L, Avalos J, Valkonen JPT, Reski R (2017) Strigolactone biosynthesis is evolutionarily conserved, regulated by phosphate starvation and contributes to resistance against phytopathogenic fungi in a moss, Physcomitrella patens. New Phytologist 216 (2):455-468. doi:10.1111/nph.14506

Delaux PM, Xie X, Timme RE, Puech-Pages V, Dunand C, Lecompte E, Delwiche CF, Yoneyama K, Becard G, Sejalon-Delmas N (2012) Origin of strigolactones in the green lineage. New Phytologist 195 (4):857-871. doi:10.1111/j.1469-8137.2012.04209.x

718 Gomez-Roldan V, Fermas S, Brewer PB, Puech-Pages V, Dun EA, Pillot JP, Letisse F,
719 Matusova R, Danoun S, Portais JC, Bouwmeester H, Becard G, Beveridge CA,
720 Rameau C, Rochange SF (2008) Strigolactone inhibition of shoot branching.
721 Nature 455 (7210):189-194. doi:10.1038/nature07271
722 Grefen C, Donald N, Hashimoto K, Kudla J, Schumacher K, Blatt MR (2010) A ubiquitin-10
723 promoter-based vector set for fluorescent protein tagging facilitates temporal
724 stability and native protein distribution in transient and stable expression
725 studies. Plant J 64 (2):355-365. doi:10.1111/j.1365-313X.2010.04322.x
726 Hamiaux C, Drummond RS, Janssen BJ, Ledger SE, Cooney JM, Newcomb RD, Snowden KC
727 (2012) DAD2 is an alpha/beta hydrolase likely to be involved in the perception of
728 the plant branching hormone, strigolactone. Curr Biol 22 (21):2032-2036.
729 doi:10.1016/j.cub.2012.08.007
730 Hiss M, Laule O, Meskauskiene RM, Arif MA, Decker EL, Erxleben A, Frank W, Hanke ST,
731 Lang D, Martin A, Neu C, Reski R, Richardt S, Schallenberg-Rudinger M, Szovenyi
732 P, Tiko T, Wiedemann G, Wolf L, Zimmermann P, Rensing SA (2014) Large-scale
733 gene expression profiling data for the model moss *Physcomitrella patens* aid
734 understanding of developmental progression, culture and stress conditions. Plant
735 J 79 (3):530-539. doi:10.1111/tpj.12572
736 Hoffmann B, Proust H, Belcram K, Labrune C, Boyer FD, Rameau C, Bonhomme S (2014)
737 Strigolactones inhibit caulonema elongation and cell division in the moss
738 *Physcomitrella patens*. PLoS One 9 (6):e99206.
739 doi:10.1371/journal.pone.0099206
740 Jang G, Dolan L (2011) Auxin promotes the transition from chloronema to caulonema in
741 moss protonema by positively regulating *PpRSL1*and *PpRSL2* in *Physcomitrella*
742 *patens*. New Phytol. doi:10.1111/j.1469-8137.2011.03805.x
743 Jiang L, Liu X, Xiong G, Liu H, Chen F, Wang L, Meng X, Liu G, Yu H, Yuan Y, Yi W, Zhao L,
744 Ma H, He Y, Wu Z, Melcher K, Qian Q, Xu HE, Wang Y, Li J (2013) DWARF 53 acts
745 as a repressor of strigolactone signalling in rice. Nature 504 (7480):401-405.
746 doi:10.1038/nature12870
747 Johnson X, Brcich T, Dun EA, Goussot M, Haurogne K, Beveridge CA, Rameau C (2006)
748 Branching genes are conserved across species. Genes controlling a novel signal in
749 pea are coregulated by other long-distance signals. Plant Physiol 142 (3):1014-
750 1026. doi:10.1104/pp.106.087676
751 Knight CD, Cove DJ, Cuming AC, Quatrano RS (2002) Moss Gene Technology, vol 2.
752 Molecular Plant Biology. Oxford University Press, Oxford
753 Li W, Nguyen KH, Watanabe Y, Yamaguchi S, Tran LS (2016) *OaMAX2* of *Orobanche*
754 *aegyptiaca* and *Arabidopsis AtMAX2* share conserved functions in both
755 development and drought responses. Biochemical and biophysical research
756 communications 478 (2):521-526. doi:10.1016/j.bbrc.2016.07.065
757 Ligerot Y, de Saint Germain A, Waldie T, Troadec C, Citerne S, Kadakia N, Pillot JP, Prigge
758 M, Aubert G, Bendahmane A, Leyser O, Estelle M, Debellé F, Rameau C (2017) The
759 pea branching *RMS2* gene encodes the PsAFB4/5 auxin receptor and is involved
760 in an auxin-strigolactone regulation loop. PLoS genetics 13 (12):e1007089.
761 doi:10.1371/journal.pgen.1007089
762 Lopez-Obando M, Conn CE, Hoffmann B, Bythell-Douglas R, Nelson DC, Rameau C,
763 Bonhomme S (2016a) Structural modelling and transcriptional responses
764 highlight a clade of *PpKAI2-LIKE* genes as candidate receptors for strigolactones
765 in *Physcomitrella patens*. Planta 243 (6):1441-1453. doi:10.1007/s00425-016-
766 2481-y

767 Lopez-Obando M, Hoffmann B, Gery C, Guyon-Debast A, Teoule E, Rameau C, Bonhomme
768 S, Nogue F (2016b) Simple and Efficient Targeting of Multiple Genes Through
769 CRISPR-Cas9 in *Physcomitrella patens*. G3 (Bethesda).
770 doi:10.1534/g3.116.033266
771 Lopez-Obando M, Ligerot Y, Bonhomme S, Boyer F-D, Rameau C (2015) Strigolactone
772 biosynthesis and signaling in plant development. Development 142 (21):3615-
773 3619. doi:10.1242/dev.120006
774 Nakamura H, Xue Y-L, Miyakawa T, Hou F, Qin H-M, Fukui K, Shi X, Ito E, Ito S, Park S-H,
775 Miyauchi Y, Asano A, Totsuka N, Ueda T, Tanokura M, Asami T (2013) Molecular
776 mechanism of strigolactone perception by DWARF14. Nat Commun 4:2613.
777 doi:10.1038/ncomms3613
778 Nelson DC, Scaffidi A, Dun EA, Waters MT, Flematti GR, Dixon KW, Beveridge CA,
779 Ghisalberti EL, Smith SM (2011) F-box protein MAX2 has dual roles in karrikin
780 and strigolactone signaling in *Arabidopsis thaliana*. Proc Natl Acad Sci U S A 108
781 (21):8897-8902. doi:10.1073/pnas.1100987108
782 Ortiz-Ramirez C, Hernandez-Coronado M, Thamm A, Catarino B, Wang M, Dolan L, Feijo
783 JA, Becker JD (2016) A Transcriptome Atlas of *Physcomitrella patens* Provides
784 Insights into the Evolution and Development of Land Plants. Mol Plant 9 (2):205-
785 220. doi:10.1016/j.molp.2015.12.002
786 Prigge MJ, Lavy M, Ashton NW, Estelle M (2010) *Physcomitrella patens* auxin-resistant
787 mutants affect conserved elements of an auxin-signaling pathway. Curr Biol 20
788 (21):1907-1912. doi:10.1016/j.cub.2010.08.050
789 Proust H, Hoffmann B, Xie X, Yoneyama K, Schaefer DG, Nogue F, Rameau C (2011)
790 Strigolactones regulate protonema branching and act as a quorum sensing-like
791 signal in the moss *Physcomitrella patens*. Development 138 (8):1531-1539.
792 doi:10.1242/dev.058495
793 Ruyter-Spira C, Kohlen W, Charnikhova T, van Zeijl A, van Bezouwen L, de Ruijter N,
794 Cardoso C, Lopez-Raez JA, Matusova R, Bours R, Verstappen F, Bouwmeester H
795 (2011) Physiological effects of the synthetic strigolactone analog GR24 on root
796 system architecture in Arabidopsis: another belowground role for strigolactones?
797 Plant Physiol 155 (2):721-734. doi:10.1104/pp.110.166645
798 Scaffidi A, Waters MT, Ghisalberti EL, Dixon KW, Flematti GR, Smith SM (2013)
799 Carlactone-independent seedling morphogenesis in Arabidopsis. Plant J 76 (1):1-
800 9. doi:10.1111/tpj.12265
801 Scaffidi A, Waters MT, Sun YK, Skelton BW, Dixon KW, Ghisalberti EL, Flematti GR, Smith
802 SM (2014) Strigolactone Hormones and Their Stereoisomers Signal through Two
803 Related Receptor Proteins to Induce Different Physiological Responses in
804 Arabidopsis. Plant Physiol 165 (3):1221-1232. doi:10.1104/pp.114.240036
805 Schaefer DG, Zryd JP (1997) Efficient gene targeting in the moss *Physcomitrella patens*.
806 Plant J 11 (6):1195-1206
807 Shen H, Luong P, Huq E (2007) The F-box protein MAX2 functions as a positive regulator
808 of photomorphogenesis in Arabidopsis. Plant Physiol 145 (4):1471-1483.
809 doi:10.1104/pp.107.107227
810 Shen H, Zhu L, Bu QY, Huq E (2012) MAX2 Affects Multiple Hormones to Promote
811 Photomorphogenesis. Mol Plant 5 (3):224-236. doi:10.1093/mp/sss029
812 Shinohara N, Taylor C, Leyser O (2013) Strigolactone can promote or inhibit shoot
813 branching by triggering rapid depletion of the auxin efflux protein PIN1 from the
814 plasma membrane. PLoS Biol 11 (1):e1001474.
815 doi:10.1371/journal.pbio.1001474

816 Soundappan I, Bennett T, Morffy N, Liang Y, Stanga JP, Abbas A, Leyser O, Nelson D
817 (2015) SMAX1-LIKE/D53 Family Members Enable Distinct MAX2-Dependent
818 Responses to Strigolactones and Karrikins in Arabidopsis. The Plant Cell 27
819 (11):3143-3159. doi:10.1105/tpc.15.00562
820 Stanga JP, Morffy N, Nelson DC (2016) Functional redundancy in the control of seedling
821 growth by the karrikin signaling pathway. Planta 243 (6):1397-1406.
822 doi:10.1007/s00425-015-2458-2
823 Stanga JP, Smith SM, Briggs WR, Nelson DC (2013) *SUPPRESSOR OF MORE AXILLARY*
824 *GROWTH2 1* controls seed germination and seedling development in Arabidopsis.
825 Plant Physiol 163 (1):318-330. doi:10.1104/pp.113.221259
826 Stirnberg P, Furner IJ, Ottoline Leyser HM (2007) MAX2 participates in an SCF complex
827 which acts locally at the node to suppress shoot branching. Plant J 50 (1):80-94.
828 doi:10.1111/j.1365-313X.2007.03032.x
829 Stirnberg P, van De Sande K, Leyser HM (2002) *MAX1* and *MAX2* control shoot lateral
830 branching in Arabidopsis. Development 129 (5):1131-1141
831 Thelander M, Nilsson A, Olsson T, Johansson M, Girod PA, Schaefer DG, Zryd JP, Ronne H
832 (2007) The moss genes *PpSKI1* and *PpSKI2* encode nuclear SnRK1 interacting
833 proteins with homologues in vascular plants. Plant Mol Biol 64 (5):559-573.
834 doi:10.1007/s11103-007-9176-5
835 Trouiller B, Schaefer DG, Charlot F, Nogue F (2006) MSH2 is essential for the
836 preservation of genome integrity and prevents homeologous recombination in
837 the moss *Physcomitrella patens*. Nucleic Acids Res 34 (1):232-242.
838 doi:10.1093/nar/gkj423
839 Ueda H, Kusaba M (2015) Strigolactone Regulates Leaf Senescence in Concert with
840 Ethylene in Arabidopsis. Plant Physiol 169 (1):138-147.
841 doi:10.1104/pp.15.00325
842 Umehara M, Hanada A, Yoshida S, Akiyama K, Arite T, Takeda-Kamiya N, Magome H,
843 Kamiya Y, Shirasu K, Yoneyama K, Kyozuka J, Yamaguchi S (2008) Inhibition of
844 shoot branching by new terpenoid plant hormones. Nature 455 (7210):195-200.
845 doi:10.1038/nature07272
846 Vismans G, van der Meer T (2016) Low-Phosphate Induction of Plastidal Stromules Is
847 Dependent on Strigolactones But Not on the Canonical Strigolactone Signaling
848 Component MAX2. 172 (4):2235-2244
849 von Schwartzenberg K, Nunez MF, Blaschke H, Dobrev PI, Novak O, Motyka V, Strnad M
850 (2007) Cytokinins in the bryophyte *Physcomitrella patens*: analyses of activity,
851 distribution, and cytokinin oxidase/dehydrogenase overexpression reveal the
852 role of extracellular cytokinins. Plant Physiol 145 (3):786-800.
853 doi:10.1104/pp.107.103176
854 Waldie T, McCulloch H, Leyser O (2014) Strigolactones and the control of plant
855 development: lessons from shoot branching. Plant J 79 (4):607-622.
856 doi:10.1111/tpj.12488
857 Walton A, Stes E, Goeminne G, Braem L, Vuylsteke M, Matthys C, De Cuyper C, Staes A,
858 Vandenbussche J, Boyer FD, Vanholme R, Fromentin J, Boerjan W, Gevaert K,
859 Goormachtig S (2016) The Response of the Root Proteome to the Synthetic
860 Strigolactone GR24 in Arabidopsis. Molecular & cellular proteomics : MCP 15
861 (8):2744-2755. doi:10.1074/mcp.M115.050062
862 Wang L, Wang B, Jiang L, Liu X, Li X, Lu Z, Meng X, Wang Y, Smith SM, Li J (2015)
863 Strigolactone Signaling in Arabidopsis Regulates Shoot Development by

Targeting D53-Like SMXL Repressor Proteins for Ubiquitination and Degradation. Plant Cell 27 (11):3128-3142. doi:10.1105/tpc.15.00605

Waters MT, Gutjahr C, Bennett T, Nelson DC (2017) Strigolactone Signaling and Evolution. Annu Rev Plant Biol. doi:10.1146/annurev-arplant-042916-040925

Waters MT, Nelson DC, Scaffidi A, Flematti GR, Sun YK, Dixon KW, Smith SM (2012) Specialisation within the DWARF14 protein family confers distinct responses to karrikins and strigolactones in Arabidopsis. Development 139 (7):1285-1295. doi:10.1242/dev.074567

Waters MT, Scaffidi A, Sun YK, Flematti GR, Smith SM (2014) The karrikin response system of Arabidopsis. Plant J 79 (4):623-631. doi:10.1111/tpj.12430

Waters MT, Smith SM (2013) KAI2- and MAX2-mediated responses to karrikins and strigolactones are largely independent of HY5 in *Arabidopsis* seedlings. Mol Plant 6 (1):63-75. doi:10.1093/mp/sss127

Woo HR, Chung KM, Park JH, Oh SA, Ahn T, Hong SH, Jang SK, Nam HG (2001) ORE9, an F-box protein that regulates leaf senescence in Arabidopsis. Plant Cell 13 (8):1779-1790

Xie X, Yoneyama K, Yoneyama K (2010) The strigolactone story. Annu Rev Phytopathol 48:93-117. doi:10.1146/annurev-phyto-073009-114453

Yamada Y, Furusawa S, Nagasaka S, Shimomura K, Yamaguchi S, Umehara M (2014) Strigolactone signaling regulates rice leaf senescence in response to a phosphate deficiency. Planta 240 (2):399-408. doi:10.1007/s00425-014-2096-0

Yamawaki S, Yamashino T, Nakanishi H, Mizuno T (2011) Functional characterization of *HY5* homolog genes involved in early light-signaling in *Physcomitrella patens*. Biosci Biotechnol Biochem 75 (8):1533-1539. doi:10.1271/bbb.110219

Yao R, Ming Z, Yan L, Li S, Wang F, Ma S, Yu C, Yang M, Chen L, Chen L, Li Y, Yan C, Miao D, Sun Z, Yan J, Sun Y, Wang L, Chu J, Fan S, He W, Deng H, Nan F, Li J, Rao Z, Lou Z, Xie D (2016) DWARF14 is a non-canonical hormone receptor for strigolactone. Nature 536 (7617):469-473. doi:10.1038/nature19073

Zhao J, Wang T, Wang M, Liu Y, Yuan S, Gao Y, Yin L, Sun W, Peng L, Zhang W, Wan J, Li X (2014) DWARF3 Participates In An SCF Complex And Associates With DWARF14 To Suppress Rice Shoot Branching. Plant & cell physiology. doi:10.1093/pcp/pcu045

Zhou F, Lin Q, Zhu L, Ren Y, Zhou K, Shabek N, Wu F, Mao H, Dong W, Gan L, Ma W, Gao H, Chen J, Yang C, Wang D, Tan J, Zhang X, Guo X, Wang J, Jiang L, Liu X, Chen W, Chu J, Yan C, Ueno K, Ito S, Asami T, Cheng Z, Lei C, Zhai H, Wu C, Wang H, Zheng N, Wan J (2013) D14-SCF(D3)-dependent degradation of D53 regulates strigolactone signalling. Nature 504 (7480):406-410. doi:10.1038/nature12878

The following Supporting Information is available for this article:

Fig. S1 Gene targeting of the *PpMAX2* gene

Fig. S2 Expression of PpMAX2 constructs in Arabidopsis

Fig. S3 PpMAX2: Phylogenetic tree, absence of intron, sequence alignment and homology model produced by I-TASSER

Fig. S4 Expression of the *PpMAX2* gene: eFPbrowser data

909 **Fig. S5** Gametophore branching in *Ppmax2*

910 **Fig. S6** Transcriptional response of the *Ppmax2* mutant to (±)-GR24

911 **Fig. S7** High doses of (±)-GR24 application mimics the *Ppmax2* mutant phenotype

912 **Table S1** 5'-3' sequences of primers used in the study

913

Fig. 1 Pattern of *PpMAX2* gene expression and subcellular localization of the protein

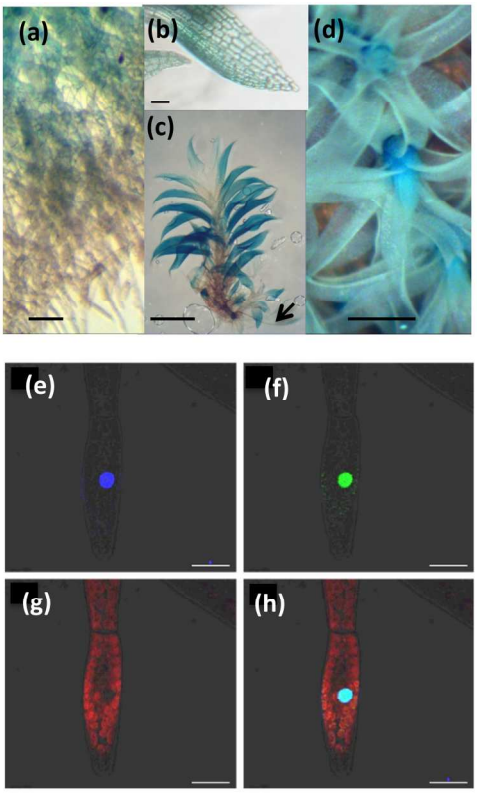

Fig.1

179x178mm (300 x 300 DPI)

Fig. 2 *Ppmax2* mutants are affected in development and show contrasting phenotype to the *Ppccd8* SL synthesis mutant.

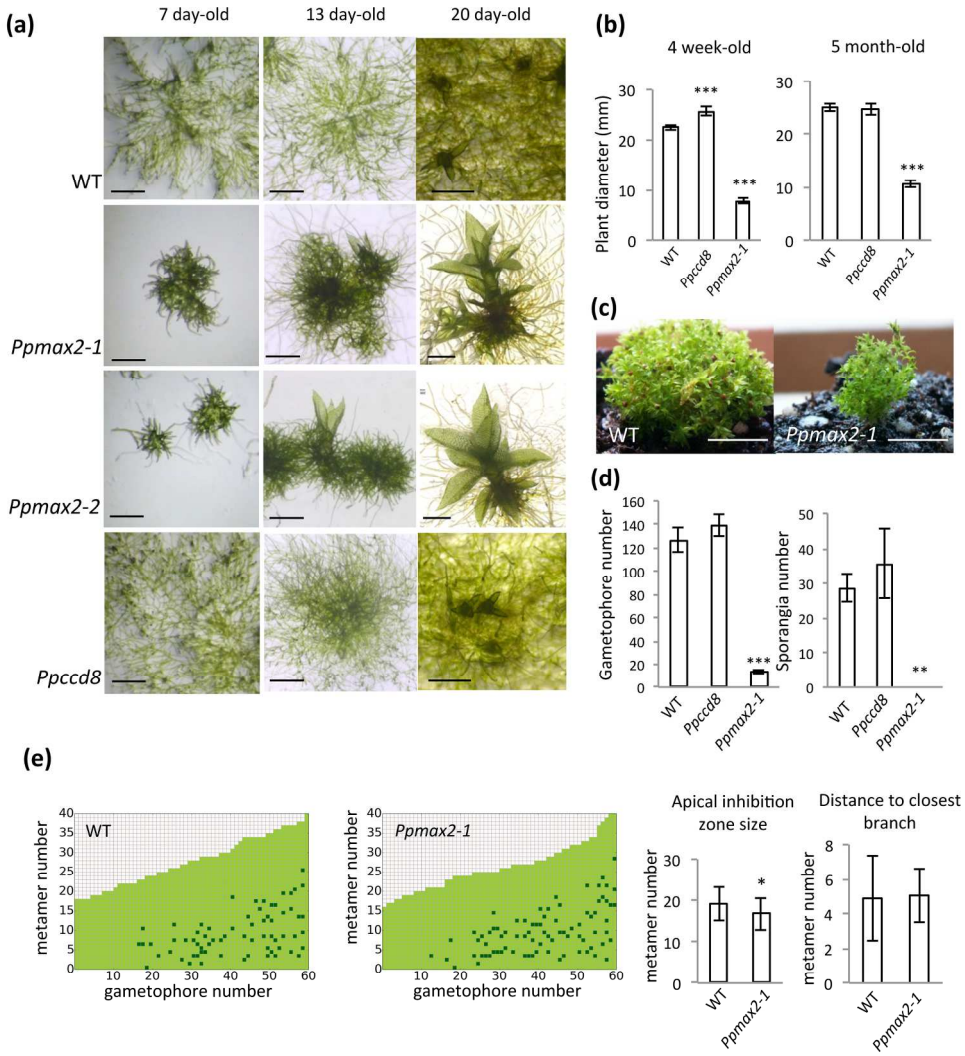

Fig.2

188x224mm (300 x 300 DPI)

Fig. 3 The *Ppmax2* mutant exudate tested on *PpCCD7* expression is similar to WT

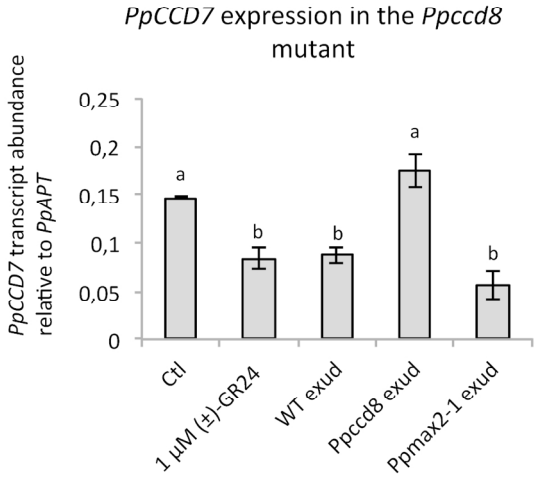

Fig.3

150x117mm (300 x 300 DPI)

Fig. 4: the *Ppmax2* mutant is sensitive to the synthetic SL GR24

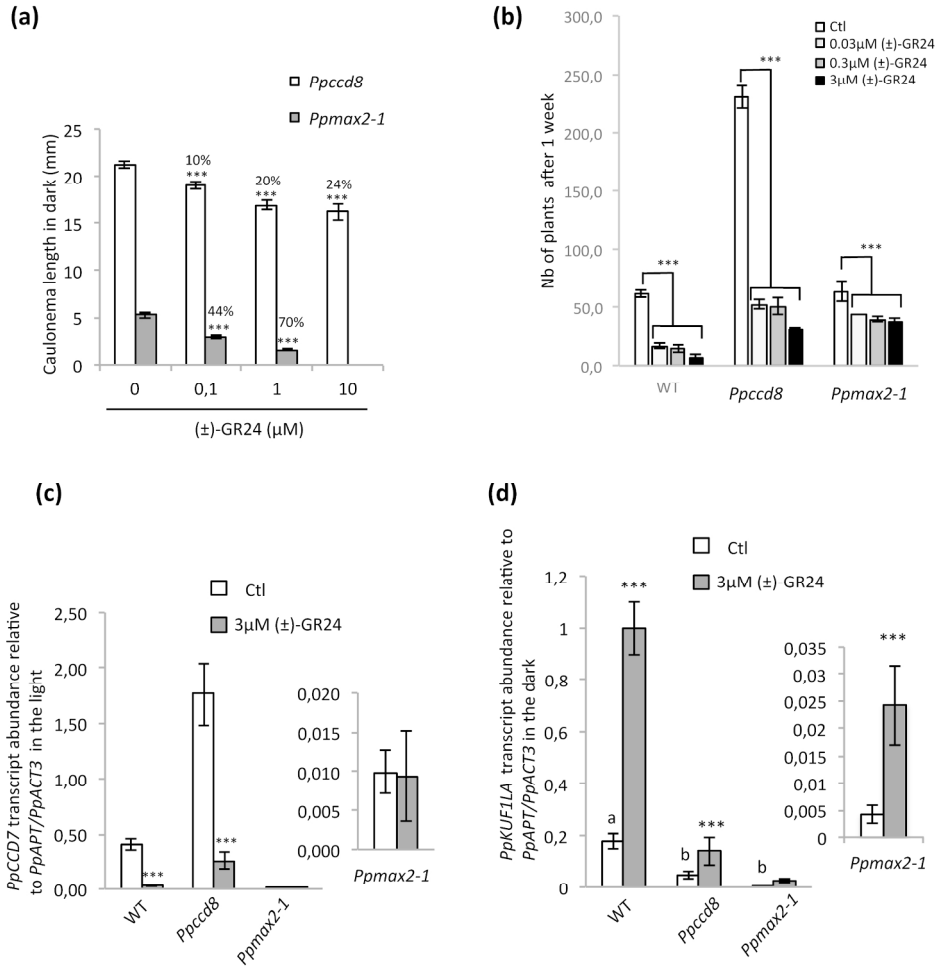

Fig.4

188x206mm (300 x 300 DPI)

Fig. 5: The *Ppmax2* mutant has impaired photomorphogenesis

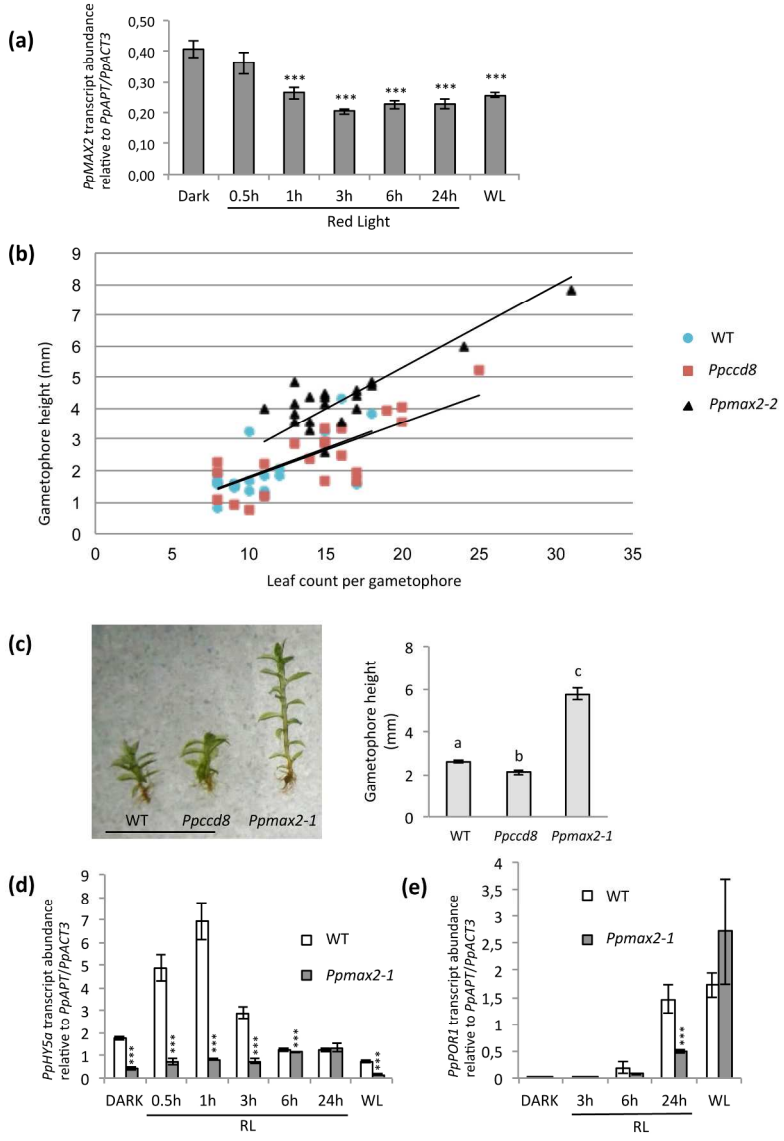

Fig.5

186x252mm (300 x 300 DPI)

Fig. 6 The *Ppmax2* mutation is epistatic to *Ppccd8*

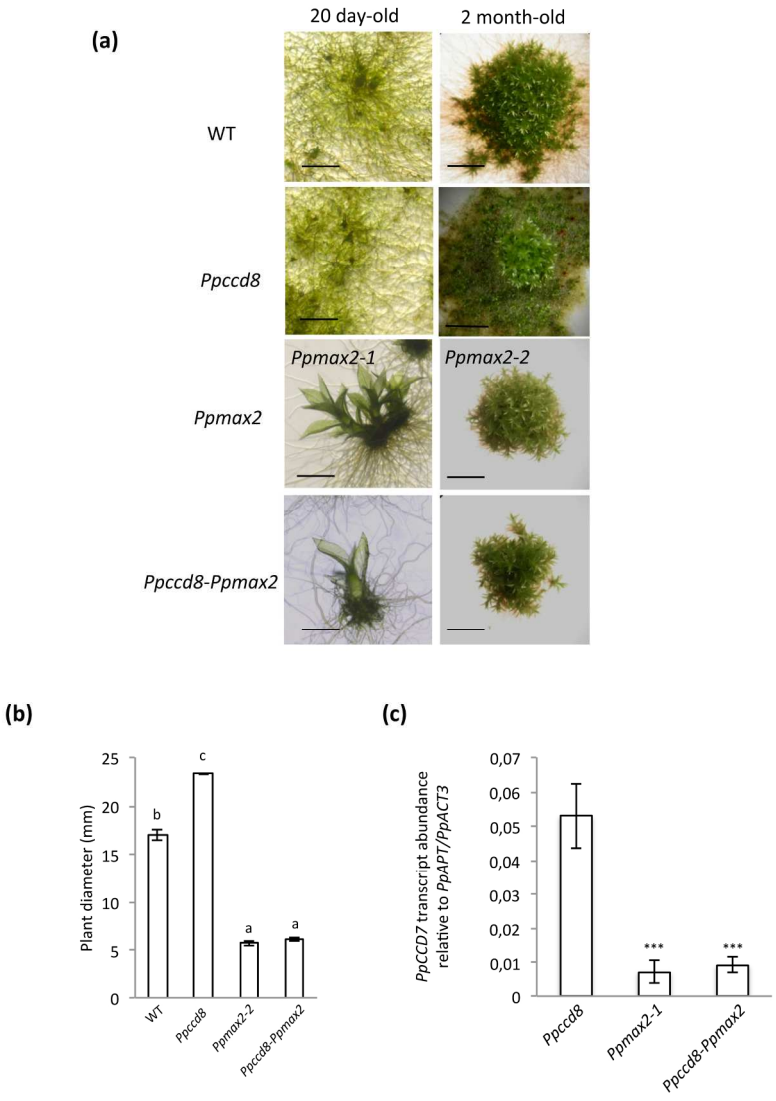

Fig.6

178x243mm (300 x 300 DPI)

Fig. 7: Expression of *PpMAX2* in the *Arabidopsis max2* mutant does not restore MAX2 function.

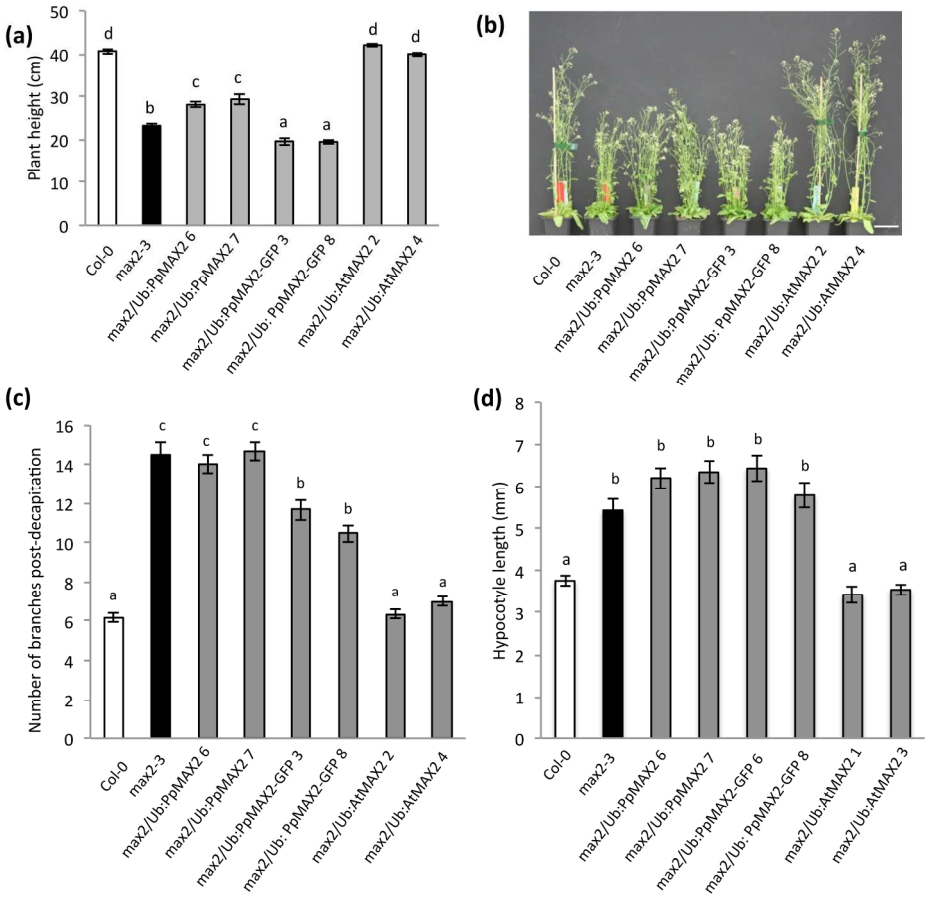

Fig.è

194x205mm (300 x 300 DPI)

Fig. 8: Model for MAX2 roles in land plants

Vascular plants

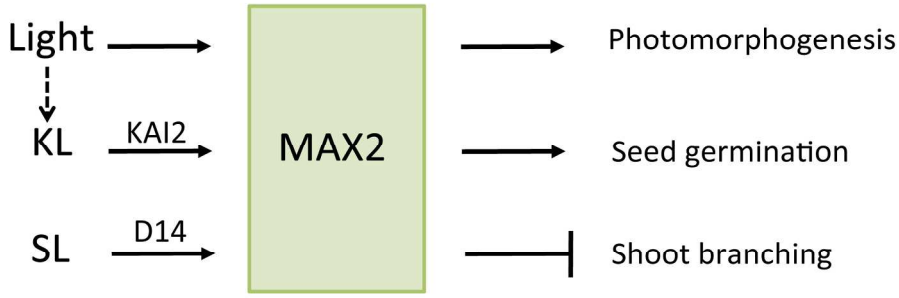

P. patens

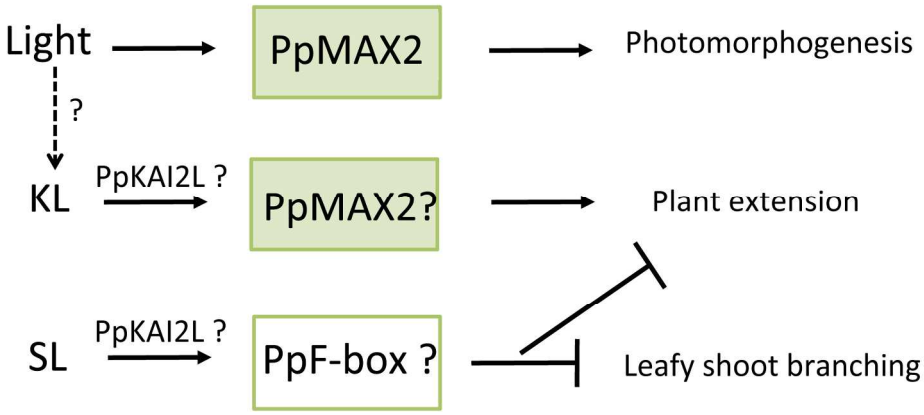

Fig.8

191x225mm (300 x 300 DPI)